Disordered Nanocrystalline Superconducting $PbMo_6S_8$ with a Very Large Upper Critical Field

H. J. Niu and D. P. Hampshire

Superconductivity Group, Department of Physics, University of Durham, Durham DH1 3LE, United Kingdom

(Received 1 October 2002; published 11 July 2003)

Large increases in the upper critical field $B_{C2}(0)$ are reported in bulk superconductors that demonstrate another novel property for nanocrystalline materials. Disordered nanocrystalline $PbMo_6S_8$ superconductors were fabricated by mechanical milling and hot isostatic pressing. Conventional $PbMo_6S_8$ has $B_{C2}(0) \sim 50$ T. The nanocrystalline materials have higher resistivity (ρ_N) and $B_{C2}(0) \sim 100$ T. The disorder produced in these nanocrystalline materials is significantly different from that produced by doping because it increases ρ_N and, hence, $B_{C2}(0)$ without significantly reducing the electronic density of states or superconducting transition temperature (T_C). Furthermore, the disorder reduces the electron mean-free path to $\sim$1 nm which is more than an order of magnitude smaller than the grain size and necessary to achieve the unprecedented increase in $B_{C2}(0)$.

DOI: 10.1103/PhysRevLett.91.027002 PACS numbers: 74.70.–b, 74.25.–q, 81.07.Bc

There is an enormous effort directed at increasing the upper critical field (B_{C2}) of the superconducting materials because B_{C2} provides a fundamental limit to the maximum field a magnet system can produce. High-energy particle accelerators and medical resonance imaging body scanners are limited by the B_{C2} for NbTi ($\sim$ 10 T). Gigahertz class nuclear-magnetic-resonance and high field laboratory magnets are limited by B_{C2} for Nb_3Sn ($\sim$ 23 T) [1]. According to BCS theory, $B_{C2}(0)$ for a superconductor at zero temperature is given by [2,3]:

$$B_{C2}(0) = R(\infty)/R(\lambda_{tr})[8.3 \times 10^{34}(\gamma T_C/S)^2 + 3.1 \times 10^3 \gamma T_C \rho_N], \quad (1)$$

where $R(\infty)/R(\lambda_{tr})$ is a strong-coupling correction close to unity, γ is the Sommerfeld constant, T_C is the critical temperature, S is the Fermi surface area, and ρ_N is the normal state resistivity. Therefore, $B_{C2}(0)$ can be increased by increasing ρ_N as long as any reduction in T_C and γ is minimized. Whether the mechanism causing the superconductivity is BCS-like or not, Ginzburg-Landau (GL) theory [4] shows that in the vicinity of a superconducting-insulating barrier, B_{C2} is increased. Hence, there is strong evidence that increasing disorder, either by increasing ρ_N or from reduced-size effects, increases B_{C2} [5].

Chemical doping or alloying has been used as the main route for improving B_{C2} of bulk superconductors by producing disorder from the lattice strain and change in the local electronic properties. Low-level doping increases ρ_N, but the enhancements of B_{C2} (4.2 K) have been small, $\sim$0.3 T in NbTi doped with Ta and Hf [6], $\sim$4 T in Nb_3Sn doped with Ti, Ta, Zr, Mo, and V [7]. Further increases in ρ_N by high-level doping depress B_{C2} rapidly [7,8]. Nevertheless, there are precedents for large increases in B_{C2} that are correlated with large increases in ρ_N. In thin films, increases in $B_{C2}(0)$ of $\sim$9 T have been reported for Nb_3Sn [3] and > 40 T for MgB_2 [9]. These increases were attributed to alloying and strain. In a metal-insulator nanocomposite synthesized by injecting indium into 56 Å pore diameter Vycor glass, an increase in $B_{C2}(0)$ by a factor of $\sim$100 has been found [10]. GL theory implies that the small crystallite size increased $B_{C2}(0)$ by reducing the electron mean-free path and, hence, the Ginzburg-Landau coherence length (ξ).

High energy mechanical milling has been used as an effective way to synthesize large quantities of disordered, nanocrystalline and amorphous powders containing large amounts of vacancies, dislocations, and grain boundaries [11,12]. Nanocrystalline bulk materials can then be obtained with different levels of disorder by subsequently compacting and heat treating the milled powder [13,14]. Nanocrystalline materials exhibit unique properties, such as increased strength, improved ductility, enhanced thermal expansion coefficient , and superior soft magnetic properties compared to conventional polycrystalline materials [13].

In this Letter, we report resistive and magnetic data in high magnetic fields and x-ray diffraction (XRD) data on disordered nanocrystalline bulk $PbMo_6S_8$. The disorder reduces the electron mean-free path in these materials to only $\sim$1 nm, which is about an order of magnitude smaller than the grain size and it also has significantly less effect on the bulk electronic density of states than doping. Hence, the superconducting coherence length in these materials is made sufficiently small to produce an unprecedented increase in $B_{C2}(0)$ for $PbMo_6S_8$ from 50 T in bulk materials up to > 100 T.

The superconducting $PbMo_6S_8$ powder used in the present study was mechanically milled for 200 h under an Ar gas atmosphere. The milled powder was consolidated using hot isostatic pressing (HIP) at different temperatures and a pressure of 2000 bars for 8 h and postannealed at 1000 °C for 40 h so as to achieve different levels of disorder and, hence, ρ_N. The details of the fabrication have been described previously [15].

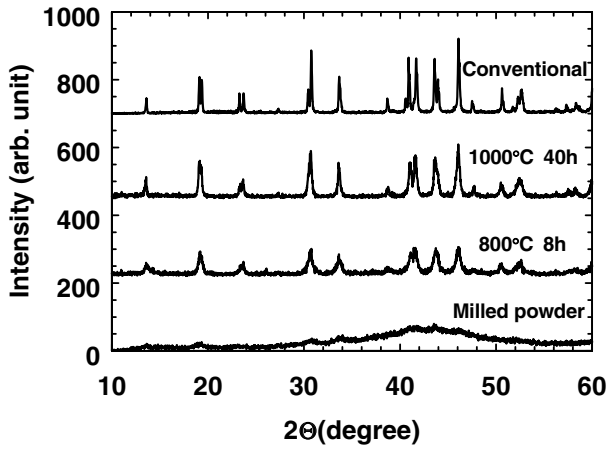

FIG. 1. XRD patterns of the conventional sample (sample 1 in Table I), the HIP and annealed samples (see samples 2 and 3 in Table I), and the 200 h milled powder. The temperature and time of the final heat treatment are labeled in the figure.

In Fig. 1, the very broad XRD peaks for the powder milled for 200 h are due to the formation of nanocrystalline and amorphous material which has been confirmed using electron diffraction analysis [15]. The average hexagonal lattice parameters (a, c) of the nanocrystalline phase determined from XRD data using a full pattern least squares "Pawley method" are much larger ($a = 9.380$ Å, $c = 12.260$ Å) than those of the conventional powder ($a = 9.198$ Å, $c = 11.495$ Å). Larger lattice parameters are usually observed when the grain size is just a few nanometers [17]. The grain size and lattice strain of the HIP samples were calculated from the XRD data using the Hall-Williamson method [18] in which $F\cos\theta/\lambda = 1/d + 4\varepsilon\sin\theta/\lambda$, where F is the difference of the full width at half maximum (FWHM) between the nanocrystalline sample and the conventional sample, d is grain size, ε is lattice strain, and θ is Bragg angle. After HIP at 800 °C, relatively sharp XRD peaks appeared due to crystallization of the amorphous phase and grain growth ($d = 20$ nm, $\varepsilon = 0.07\%$, $a = 9.220$ Å, and $c = 11.455$ Å). With increasing temperature of annealing, the XRD peaks became even sharper but still broader than those of the conventional sample (sample 1). Hence, disordered nanocrystalline bulk samples (samples 2 and 3) with grain sizes between 20 and 90 nm were obtained, as shown in Table I.

Table I presents the values of the normal state resistivity at 16 K [ρ_N (16 K)], room-temperature resistivity ratios (RRR), and critical temperature (T_C). The values of T_C determined using the criterion of $0.95\rho_N$ systematically decrease from 15.05 K for sample 1 to 12.30 K for sample 3 correlated with a decrease in RRR and a large increase in ρ_N (16 K) from 80 to 680 $\mu\Omega$ cm.

The magnetization of the samples was measured in magnetic fields up to 12 T at temperatures up to ~15 K using a commercial vibrating sample magnetometer.

Figure 2 shows the magnetization magnetic field (M-H) curves obtained for samples 1 and 3 after subtracting the background. The reversible region of the M-H loops at the highest fields (typically above 9 T) was extrapolated to zero magnetization at each temperature to obtain experimental values of $\partial M/\partial B$, $B_{C2}(T)$, and $\partial B_{C2}/\partial T|_{T_C}$. $B_{C2}(0)$ was then calculated using Werthamer-Helfand-Hohenberg theory [19]:

$$B_{C2}(0) = -0.7T_C\partial B_{C2}/\partial T|_{T_C}. \quad (2)$$

The Ginzburg-Landau parameter, κ, was calculated using the Abrikosov equation [20]:

$$\mu_0 M = -\frac{(B_{C2} - B)}{(2\kappa^2 - 1)\beta_A}\Bigg|_{B_{C2}}, \quad (3)$$

where $\beta_A = 1.16$. The value of the coherence length, $\xi(0)$, at zero temperature was calculated by employing the Ginzburg-Landau relations:

TABLE I. Processing conditions, grain size (d), normal state resistivity (ρ_N), residual resistivity ratio (RRR), Sommerfeld constant (γ), and superconducting parameters.

No.	Type	d (nm)	ρ_N(16 K) ($\mu\Omega$ cm)	RRR[a]	T_C[b] (K)	$-\partial B_{C2}/\partial T$ (TK^{-1})	$B_{C2}(0)$ (T)	κ	$\xi(0)$[c] (nm)	γ ($JK^{-2}m^{-3}$)	$B_C(0)$ (T)	J_C[d] (10^8 Am^{-2})
1	Conventional	2000[e]	80	7.8	15.05	4.6	45	125	2.2	380	0.22	6.5
2	Milled	90	360	2.0	14.40	7.3	65	240	1.9	250	0.16	20
3	Milled	20	680	1.4	12.30	14.1	110	520	1.4	200	0.13	19
4[f]	Doped	2000[e]	280	3.3	14.80	5.1	50	160	2.1	270	0.19	12
5[f]	Doped	2000[e]	800	1.6	13.65	5.0	45	260	2.3	100	0.10	6.0

[a] $RRR = \rho_N(290\text{ K})/\rho_N(16\text{ K})$.
[b] T_C was determined by resistivity measurement using the criterion of $0.95\rho_N$—all superconducting parameters were calculated with T_C obtained from the magnetic measurements.
[c] $\xi(0)$ is the coherence length at zero temperature.
[d] J_C at 4.2 K and zero magnetic field was calculated from the magnetic hysteresis data using the critical state model [16].
[e] The average grain size was determined using scanning electron microscopy.
[f] Samples 4 and 5 are the Cu doped samples, $Pb_{1-x}Cu_{1.8x}Mo_6S_8$ with $x = 0.02$ and 0.10, respectively, and HIP at the pressure of 2000 bars and the temperature of 800 °C for 8 h.

$$B_{C2}(T) = \frac{\Phi_0}{2\pi\xi^2(T)}\Big|_{T_C}, \quad (4)$$

$$\xi(T) = \xi(0)(1 - T/T_C)^{-0.5}|_{T_C}, \quad (5)$$

where $\Phi_0 = 2.07 \times 10^{-15}$ Wb [21].

The Sommerfeld constant (γ) and the thermodynamic critical field at zero temperature, $B_C(0)$, were calculated using a Ginzburg-Landau relation and results from microscopic theory in the BCS limit [22]:

$$B_{C2}(T) = \sqrt{2}\kappa(T_C)B_C(T)|_{T_C}, \quad (6)$$

$$\left(\frac{\partial B_C(T)}{\partial T}\right)\Big|_{T_C} = -1.20\mu_0^{1/2}\gamma^{1/2}, \quad (7)$$

$$B_C(0) = 0.69\mu_0^{1/2}\gamma^{1/2}T_C. \quad (8)$$

Table I shows the parameters obtained. Sample 3 has a substantially higher value of $-\partial B_{C2}/\partial T|_{T_C}$ (14.1 TK^{-1}) than sample 1 (4.6 TK^{-1}) and a commensurately higher value of $B_{C2}(0)$ (110 T compared to 45 T). In the nanocrystalline samples, κ increases and $\xi(0)$ decreases with increasing ρ_N. Importantly, the disorder reduces the value of $\xi(0)$ to a much smaller value than the grain size (d), which indicates a high level of intragranular defects and is consistent with the change in lattice parameters determined from XRD data and reported for nanocrystalline materials that have been supersaturated with vacancies [17]. The values of $B_C(0)$ for the nanocrystalline and standard polycrystalline samples are similar and confirm that the higher values of $B_{C2}(0)$ are bulk properties. Despite the large range of reversible magnetization (see Fig. 2), the value of critical current density (J_C) at 4.2 K and zero field is $\sim 2.0 \times 10^9$ Am^{-2} as shown in Table I, the highest reported in bulk materials of $PbMo_6S_8$. The high value of J_C is believed to be due to the increase in intragranular defects and grain boundaries acting as pinning centers [23] and improved intergranular connectivity.

Resistive measurements made on samples 1 and 3 in magnetic fields up to 15 T and temperatures 6 to 16 K are shown in Fig. 3. For sample 1, increasing the magnetic field results in a shift of the entire resistive transition to lower temperature, characteristic of conventional low temperature superconductors. In contrast, the high-resistivity nanocrystalline sample 3 has a nearly constant onset temperature for superconductivity with a broadened transition in high fields characteristic of the Y-, Bi-, and Tl-cuprate high-temperature superconductors [24]. If an arbitrary resistive criterion of, for instance, $0.95\rho_N$ is used, the value of $B_{C2}(0)$ is $\sim$68 T for sample 3, much higher than 53 T for sample 1. However, as reported for the high-temperature superconductor $YBa_2Cu_3O_7$, there was no distinct identifiable feature of B_{C2} in the resistive data [24].

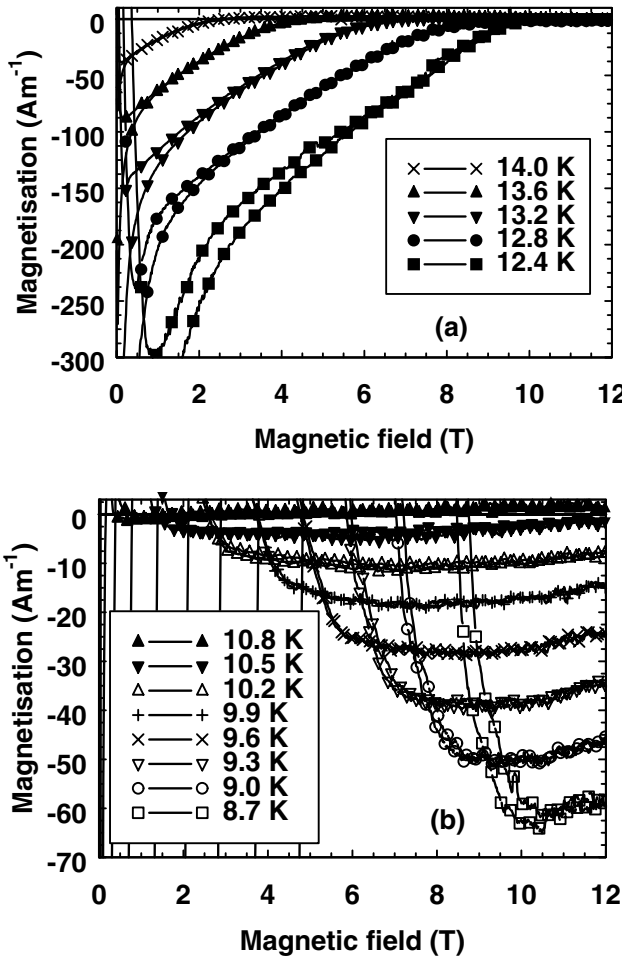

FIG. 2. *M-H* curves measured using a commercial vibrating sample magnetometer at different temperatures and magnetic fields up to 12 T. The backgrounds measured at a temperature above T_C were subtracted from the data. The upper critical field B_{C2} was determined by linearly extrapolating the reversible region to the field where magnetization becomes zero. (a) sample 1, (b) sample 3; the linear extrapolation was performed at fields larger than 9 T for all temperatures except for 10.8 K.

In order to compare the nanocrystalline samples with doped samples, Table I lists the superconducting parameters of two Cu doped $PbMo_6S_8$ samples, $Pb_{1-x}Cu_{1.8x}Mo_6S_8$ with $x = 0.02$ (sample 4) and 0.10 (sample 5), respectively. The values of ρ_N (16 K) increase with increasing Cu content. A combination of relatively high $\rho_N(16\text{ K}) = 800\ \mu\Omega\,\text{cm}$ and $T_C = 13.65$ K were obtained in the Cu doped sample 5. However, sample 4 shows only a slight increase in $B_{C2}(0)$ to 50 T. Further increasing Cu content to $x = 0.10$ leads to a decrease of $B_{C2}(0)$ to 45 T (sample 5). A similar behavior with doping has also been found in Nb_3Sn [7,8].

The reduction in γ, shown in Table I, for the milled and doped samples compared to the conventional sample is consistent with a very general consideration of the uncertainty relation $\Delta E \Delta\tau = \hbar$ which suggests that

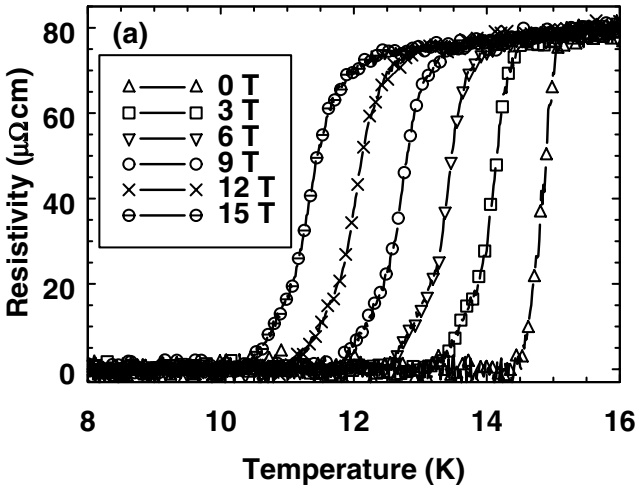

FIG. 3. Resistive superconducting transitions measured at magnetic fields up to 15 T. (a) Sample 1; (b) sample 3.

increased disorder will tend to smear out and, hence, reduce any peak in the density of states and γ [25]. Strong electron-phonon coupling, in which T_C is less sensitive than weak coupling to changes in the electron density of states, is well established in Chevrel phase compounds [26]. Hence, given the effect of disorder on γ, the relatively small reduction in T_C found in all the samples may result from the strong coupling in these materials and possibly an increase in the electron-phonon coupling as found in other superconductors [27] produced by phonon softening [7]. If the Cu doped sample 5 in Table I is compared with the nanocrystalline sample 3, they have similar ρ_N and T_C, but γ is different by a factor of $\sim$2. Hence, nanocrystalline disorder is significantly more effective than doping at increasing scattering without reducing the electronic density of states. Indeed, it can be noted that an enhancement of γ has been predicted by theory for some nanocrystalline materials [28,29] and found using low temperature specific heat measurements [13,29].

Intragranular defects found in the disordered nanocrystalline materials produce electron scattering on a smaller scale than the grain size. The disorder in the nanocrystalline materials has a significantly less detrimental effect on the electronic density of states than that produced by doping. Future research into metastable materials may yet provide a new class of highly disordered superconductors with very high $B_{C2}(0)$.

We would like to thank Dr. J. S. O. Evans for the XRD measurement. This work was supported by EPSRC U.K. Grant No. GR/M85517.

[1] H. Krauth, in *Handbook of Applied Superconductivity*, edited by B. Seeber (IOP, London, 1998), Vol. 1, p. 397.
[2] J. Bardeen, L. N. Cooper, and J. R. Schrieffer, Phys. Rev. **108**, 1175 (1957).
[3] T. P. Orlando *et al.*, Phys. Rev. B **19**, 4545 (1979).
[4] V. L. Ginsburg and L. D. Landau, Zh. Eksp. Teor. Fis. **20**, 1064 (1950) [Sov. Phys. JETP **36**, 1364 (1959)].
[5] J. P. Hurault, Phys. Lett. **20**, 587 (1966).
[6] D. G. Hawksworth and D. C. Larbalestier, IEEE Trans. Magn. **17**, 49 (1981).
[7] M. Suenaga *et al.*, J. Appl. Phys. **59**, 840 (1986).
[8] T. P. Orlando *et al.*, IEEE Trans. Magn. **17**, 368 (1981).
[9] C. B. Eom *et al.*, Nature (London) **411**, 558 (2001).
[10] M. J. Graf, T. E. Huber, and C. A. Huber, Phys. Rev. B **45**, 3133 (1992).
[11] C. C. Koch, Nanostruct. Mater. **2**, 109 (1993).
[12] M. Murayama *et al.*, Science **295**, 2433 (2002).
[13] H. Gleiter, Prog. Mater. Sci. **33**, 223 (1989).
[14] H. Gleiter, Acta Mater. **48**, 1 (2000).
[15] H. J. Niu and D. P. Hampshire, Physica (Amsterdam) **372C–376C**, 1145 (2002).
[16] C. P. Bean, Rev. Mod. Phys. **36**, 31 (1964).
[17] X. D. Liu *et al.*, J. Phys. Condens. Mater. **6**, L497 (1994).
[18] G. Ziegler, Powder Metall. Int. **10**, 70 (1978).
[19] N. R. Werthamer, E. Helfand, and P. C. Hohenberg, Phys. Rev. **147**, 295 (1966).
[20] A. A. Abrikosov, Sov. Phys. JETP **5**, 1174 (1957).
[21] D. P. Hampshire, in *Handbook of Superconducting Materials*, edited by D. Cardwell (IOP, Bristol, 2002).
[22] F. Marsiglio and J. P. Carbotte, Phys. Rev. B **33**, 6141 (1986).
[23] D. Dew-Hughes, Philos. Mag. B **55**, 459 (1987).
[24] U. Welp *et al.*, Phys. Rev. Lett. **62**, 1908 (1989).
[25] J. E. Crow *et al.*, Phys. Lett. **30A**, 161 (1969).
[26] M. Furuyama, N. Kobayashi, and Y. Muto, Phys. Rev. B **40**, 4344 (1989).
[27] W. L. McMillan, Phys. Rev. **167**, 331 (1968).
[28] V. E. Kenner and R. E. Allen, Phys. Rev. B **11**, 2858 (1975).
[29] O. Vergara, D. Heitkamp, and H. v. Lohneysen, J. Phys. Chem. Solids **45**, 251 (1984).